THE AMERICAN SOCIETY OF MECHANICAL ENGINEERS
345 E. 47th St., New York, N.Y. 10017

98-GT-127



# APPLICATION OF A THREE-DIMENSIONAL INVERSE METHOD TO THE DESIGN OF A CENTRIFUGAL COMPRESSOR IMPELLER

**Alain Demeulenaere**
Numeca International
avenue F. Roosevelt, 5
1050 Brussels
Belgium

**Olivier Léonard**
Université de Liège
rue E. Solvay, 21 (C3)
4000 Liège
Belgium

**René Van den Braembussche**
von Karman Institute
chaussée de Waterloo, 72
1640 Rhode-Saint-Genese
Belgium



## ABSTRACT

The use of a three-dimensional Euler inverse method for the design of a centrifugal impeller is demonstrated.

Both the blade shape and the endwalls are iteratively designed. The meridional contour is modified in order to control the mean velocity level in the blade channel, while the blade shape is designed to achieve a prescribed loading distribution between the inlet and the outlet.

The method solves the time dependent Euler equations in a numerical domain of which some boundaries (the blades or the endwalls) move and change shape during the transient part of the computation, until a prescribed pressure distribution is achieved on the blade surfaces.

The method is applied to the design of a centrifugal compressor impeller, whose hub endwall and blade surfaces are modified by the inviscid inverse method. The real performance of both initial and modified geometries are compared through three-dimensional Navier-Stokes computations.

## NOMENCLATURE

| | |
|---|---|
| $N_b$ | number of blades |
| $p$ | static pressure |
| $r$ | radius |
| $R_c$ | curvature radius of meridional streamlines |
| $V$ | absolute velocity |
| $W$ | relative velocity |
| $\beta$ | blade-to-blade flow angle |
| $\delta$ | meridional angle (from axial direction) |
| $\rho$ | density |
| $\omega$ | speed of rotation |

**Subscripts**

| | |
|---|---|
| $m$ | meridional direction |
| $n$ | normal direction |
| $\theta$ | circumferential direction |

**Superscripts**

| | |
|---|---|
| $n$ | value at the time step $n$ |
| $req$ | required value |

## INTRODUCTION

Computational Fluid Dynamics (CFD) has now matured to the point at which it is widely accepted as a key tool for aerodynamic design. The principles underlying the design and implementation of robust schemes which can accurately resolve compressible flows around complex geometries are now quite well established. CFD is however still not being exploited as one would expect in the design process. Most designers still adopt a 'trial and error' approach, analysing the current design, and modifying it as a function of the computational results or the experimental data, according to empirical rules or to their own experience. This approach can be time consuming, and does not allow for the highest performance, such as those of transonic shock free blade sections.

A more efficient definition of optimized three-dimensional designs is possible by means of optimization and/or inverse methods, which allow for the generation of geometries achieving a prescribed performance.

Numerical optimization methods iteratively modify a set of geometrical parameters, until an error function which expresses the difference between desired and actual performance is minimized. These methods can be combined with any type of flow solver, and can easily handle geometrical and aerodynamic constraints. However they usually have the disadvantage of being expensive in terms of CPU time.

Inverse methods define the blade shape for a prescribed Mach number or pressure distribution. They use physical models to derive the geometrical changes required for achieving the prescribed performance, and are therefore

Presented at the International Gas Turbine & Aeroengine Congress & Exhibition
Stockholm, Sweden — June 2–June 5, 1998

more efficient. The CPU time required for designing a new geometry with these methods is of the same order of magnitude as for the analysis of a given geometry (usually 2 or 3 times longer), while optimization methods sometimes require hundreds of analyses.

On the other hand inverse methods require the definition of a target pressure distribution, which is supposed to be optimized, and must face the problem of existence of a solution. As soon as the flow becomes compressible, it has never been possible to guarantee that any feasible geometry corresponds to a given target pressure distribution. Moreover, if a solution exits, it does not necessarily meet all the design requirememts, which can be of mechanical nature (blade thickness, weight, inertia) or aero- and thermodynamic nature (pressure ratio, mass flow, turning angle).

Although it is now better understood in the field of turbomachinery (Léonard and Van den Braembussche, 1992b), it must however be recognized that this problem of existence of a solution is sometimes responsible for the difficult integration of inverse methods into industrial design processes. One often has to try several target pressure distributions before the one that leads to an acceptable solution is found. Moreover many inverse methods tend to "blow up" as long as the target is 'inappropriate'. This further complicates the target definition, as no feed-back is given on how the target should be modified. An inverse method needs years of development and experience to be sufficiently mature so that it can be used in industry.

The method presented in this paper is the result of 9 years of development. Léonard and Van den Braembussche (1992a) developed a two-dimensional Euler inverse method, and applied it to the design of transonic compressor and turbine cascades. Demeulenaere and Van den Braembussche (1996) extended the method to three dimensions.

The method has recently been reformulated, in order to be applicable to both viscous and inviscid problems (Demeulenaere and Léonard, 1997). The new version offers several advantages when compared to the previous one. It is faster in many cases, and gives a better control of the geometry modifications, which facilitates the definition of the target (Demeulenaere, 1997). The constraints imposed on the blade thickness and the outlet flow angle can automatically be taken into account, respectively by imposing the pressure on a part of the blade surface (the rest of the surface being defined from an imposed thickness distribution), and by introducing a degree of freedom in the target. This degree of freedom allows for a direct control of the surface of the pressure diagram, and hence of the flow deviation by the blades.

## RADIAL TURBOMACHINERY DESIGN

The design of turbomachinery stages is often based on the well-known S1-S2 decomposition. Throughflow calculations determine a set of streamsurfaces and the streamtube thickness evolution throughout the stage. Blade-to-blade calculations are performed on the axisymmetric surfaces. These two problems are solved iteratively, and if the coupling is not too strong, convergence is quite rapidly obtained.

Centrifugal compressors usually have long blades with increasing pitch toward the outlet, which makes the streamsurfaces less axisymmetric, and is responsible for the lower accuracy of the S1-S2 approach. Another main characteristic of centrifugal impellers is the strong curvature of the meridional streamlines. This curvature induces a centrifugal force, which is opposite to the centrifugal force caused by the swirl of the flow. The equilibrium between these forces results in the pressure gradient in the direction $n$ normal to the meridional streamlines:

$$\frac{1}{\rho}\frac{\partial p}{\partial n} = \frac{(W_m \tan\beta - \omega r)^2}{r}\cos\delta - \frac{W_m^2}{R_c} \qquad (1)$$

where $r$, $\delta$ and $R_c$ refer respectively to the radial position, the direction (with respect to the axis of rotation) and the radius of curvature of the meridional streamlines. The relation (1) together with the continuity equation determines the meridional streamtube distribution. Any change of blade shape induces significant changes of the blade-to-blade flow angle ($\beta$), and hence of this meridional equilibrium. On the other hand, the endwalls have a direct influence on the curvature radius and on the relative velocity level $W$ in the channel.

In radial machines, part of the work is done through the flow deflexion by the blades, while the other part results from the radius change, defined by the shape of the endwalls. The blade-to-blade pressure gradient is related to the evolution of the swirl $rV_\theta$ throughout the meridional section of the machine:

$$\frac{\Delta p_{SS-PS}}{\rho} = \frac{2\pi}{N_b}\vec{W}.\vec{\nabla}(rW_m\ \tan\beta - \omega r^2) \qquad (2)$$

where $N_b$ refers to the number of blades, and $\vec{W}$ is the relative velocity vector.

The conclusion that can be drawn from this short introduction is that both the endwalls and the blades influence the flow in radial components, and that their effects are strongly coupled, which slows down the convergence of a classical quasi-3D design approach. A more efficient design procedure for radial impellers must therefore be based on the three-dimensional flow equations, and must include the design of the endwalls.

In this paper, it will be shown that the 3D Euler inverse method previously published by the authors (Demeulenaere and Van den Braembussche, 1996) can be used for this purpose. The method is based on the inviscid flow equations, and is therefore unable to predict the large secondary flows and flow separations usually occuring at the outlet of centrifugal impellers. It is however well accepted that secondary flows do not influence the pressure distribution along the blade walls that much (except if boundary layer separation occurs). An inverse method based on a pressure target distribution is therefore valid for impellers that are not too heavily loaded.

## DESCRIPTION OF THE INVERSE DESIGN STRATEGY FOR RADIAL MACHINES

The thickness of radial impeller blades being usually imposed from mechanical considerations, only the shape of the camber line of the blades can be re-designed. In this case it is impossible to control the pressure distribution on both sides of the blade surface, because this would lead to an over-determined (and hence ill-posed) problem. One degree of freedom is missing to obtain a full control of the pressure distribution, but it can be (partially) recovered by controlling also the shape of the hub and/or tip endwalls.

The strategy that we propose here is based on the idea that the blades and the endwalls play complementary roles. It is widely accepted that the meridional velocity variation is more or less fixed by the hub and shroud contours, whereas the blade-to-blade loading distribution within the impeller mainly depends on the shape of the blades. Many turbomachinery manufacturers agree with this approach, and use it succesfully to design their machines (Casey et al, 1992, Van den Braembussche et al, 1993).

We decided to perform successively some meridional contour and blade shape (camber line) modifications, in order to control respectively the mean velocity level and the blade loading distributions. For comparison purpose, the Circulation method (Hawthorne et al, 1984), that has been used to design radial components, defines the blade shape corresponding to a prescribed streamwise distribution of swirl or blade-to-blade pressure gradient (Zangeneh, 1993, Dang, 1997). This method however does not offer the possibility to design the endwalls, and therefore does not provide any control of the velocity level, and hence of the diffusion along the blades. Recently Zangeneh (1997) presented preliminary results of a new version of the method, including the design of the endwalls.

## THE BLADE DESIGN METHOD

The blade camber line is designed with the 3D inverse method previously published by the authors (Demeulenaere and Léonard, 1997).

This method is organised as a time marching procedure, in which the walls move during the transient part of the calculatinn. Each iteration is decomposed into two steps. The first step modifies the blade shape with a transpiration method, the transpiration flux computation being based on the permeable wall concept. The second step cnnsists of updating the flow field, taking into account the blade wall movement during the time stepping.

The computer cnde is based on a high resolution three-dimensional finite volume Euler solver. An upwind-biased evaluation of the advective fluxes allows for sharp shock wave capturing, and low numerical entropy generatinn. The wall boundary conditions make use of the compatibility relations, in order to respect the hyperbolic character of the Euler equations. Non reflecting boundary conditions are applied along the inlet/outlet boundaries, in order to avoid spurious reflection of the incident waves (Giles, 1989). An

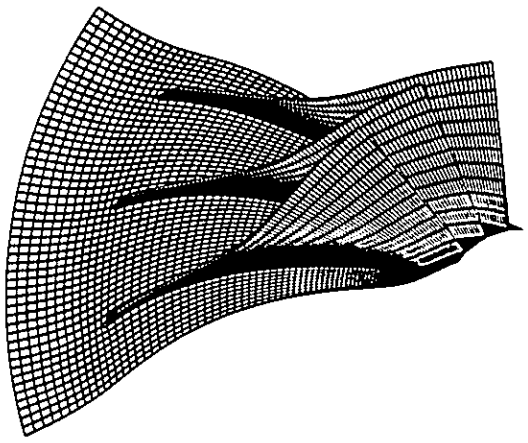

**Fig. 1: 3D View of the initial design**

explicit 4-step Runge-Kutta algorithm is used to integrate the equations in time toward the steady-state.

The blade is re-designed for a prescribed streamwise distribution of suction to pressure side pressure difference. The mean pressure level is not explicitly controlled during this step, but as already pointed out, it is mainly influenced by the shape of the endwalls. It is therefore expected that the mean velocity distributinn remains more or less constant as long as only the blade walls are modified.

The inverse method is organised exactly as if both suction and pressure sides were re-designed, but as the blade thickness is maintained constant, the pressure distributions imposed on both sides of the blades are iteratively modified, according to the prescribed value of pressure difference, and according to the average pressure level resulting from the previous time iteration:

$$p_{\text{walls}}^{n+1} = p_{\text{av}}^{n} \pm \frac{\Delta p^{\text{req}}}{2} \qquad (3)$$

## THE ENDWALL DESIGN METHOD

The design of the endwalls is based on the same inverse strategy, except that this time the two-dimensional circumferentially-averaged Euler equations are solved. This axisymmetric computation is performed in the meridional plane, and can be seen as a three-dimensional calculation performed with only one cell in the circumferential direction.

The $\theta$-mnmentum equatinn is not solved, but is replaced by the hypothesis that the average blade-to-blade flow angle distribution equals the one resulting from the 3D computation around the previous geometry, which automatically takes the slip factor effect into account. The advective fluxes through the blade surfaces reduce to the pressure forces,

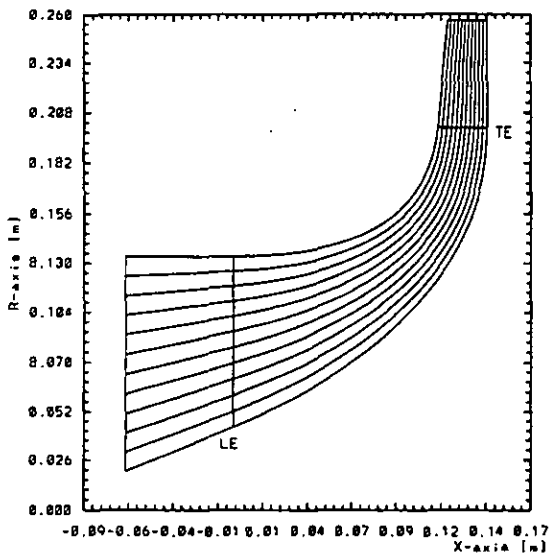


Fig. 2: Meridional view

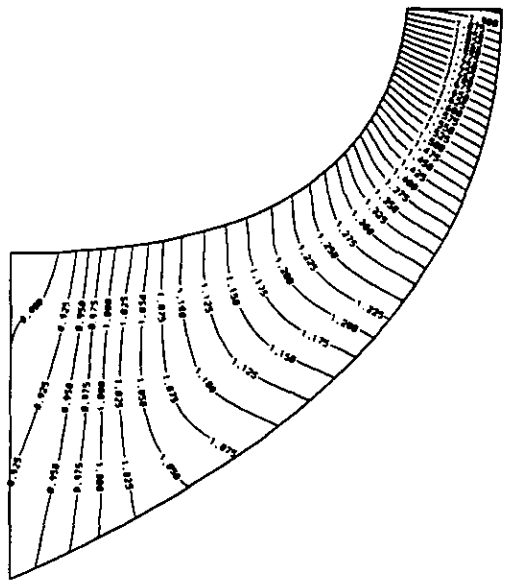

Fig. 3: Initial design - Circumf.-averaged pressure distribution in the channel - 3D flow calculation

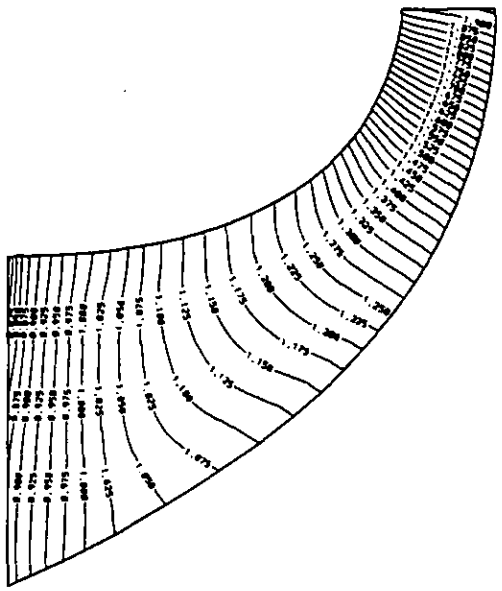

Fig. 4: Initial design - Circumf.-averaged pressure distribution in the channel - Meridional flow calculation

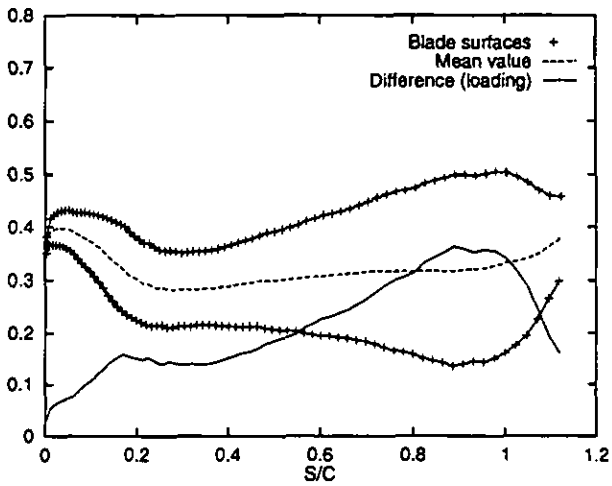


Fig. 5: Isentropic Mach number and loading distributions around the initial blade - Hub section

whose components in the axial and radial directions are introduced as source terms in the formulation. The blade-to-blade pressure difference is computed from the meridional distribution of swirl, through relation (2). In this relation, the axial and radial derivatives of the swirl are iteratively computed, using the Green theorem:

$$\frac{\partial(rV_\theta)}{\partial x} = \frac{1}{Vol}\oint (rV_\theta) n_x dS \qquad (4)$$

$$\frac{1}{r}\frac{\partial(rV_\theta)}{\partial r} = \frac{1}{Vol}\oint V_\theta n_r dS \qquad (5)$$

In the analysis mode, the usual inviscid slip condition is imposed along the hub and shroud endwalls, and the results obtained in terms of average pressure distribution show a satisfactory agreement with the 3D calculations, as shown by figures 3 and 4 for the centrifugal impeller whose redesign will be presented in the next section.

In the inverse mode, the average pressure between pressure and suction side is prescribed along the hub and/or tip endwalls, giving rise to a distribution of normal velocities along the wall, which is used to modify the endwalls by means of a transpiration method. The inlet section is kept unchanged, and all discretization points defining the

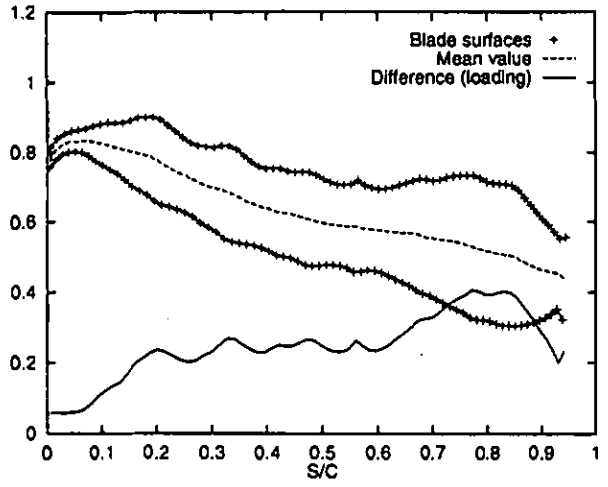


**Fig. 6: Isentropic Mach number and loading distributions around the initial blade - Tip section**

endwalls are then displaced along the local normal distance, applying the mass conservation principle to compute the amplitude of the displacements. As this approach does not allow for a direct control of the position of the hub and/or shroud outlet points (moving in the axial direction), one may expect some stability problems when large modifications are undertaken. However, when the method is used in order to improve an initial design, the inlet/outlet pressure levels are usually not modified by the user. The mass flow then remains unchanged, and nn convergence problems are encountered.

## EXAMPLE OF CENTRIFUGAL IMPELLER DESIGN

The initial geometry that we intend to re-design is shown in figure 1, while figure 2 shows the meridional cross section. This geometry has been designed with a rapid one-dimensional method. The 20 twisted blades rotate at 18,000 RPM. Figure 2 also shows the 12 axisymmetric surfaces on which periodic H-grids have been generated to discretise the numerical domain. The flow conditions that have been considered are the following: mass flow= 7 kg/s, $\pi$ (total pressure ratio)= 2.66, $\tau$ (total temperature ratio)= 1.32.

A three-dimensional Euler computation has been performed around the initial geometry, for a zero inlet swirl, and an outlet isentropic Mach number of 0.755. The isentropic Mach number distributions along the hub and tip blade sections are shown in figures 5 and 6. Four curves are plotted on each figure, showing not only the Mach nnmher distributions along the suction and pressure sides, but also the average value and the pressure-to-suction side Mach number difference. The hub velocity distribution is clearly not optimal, with a significant deceleration in the first 30%, which is due to the concavity of the hub contour downstream of the leading edge. The velocity distribution along the tip section is acceptable, but the loading shows some

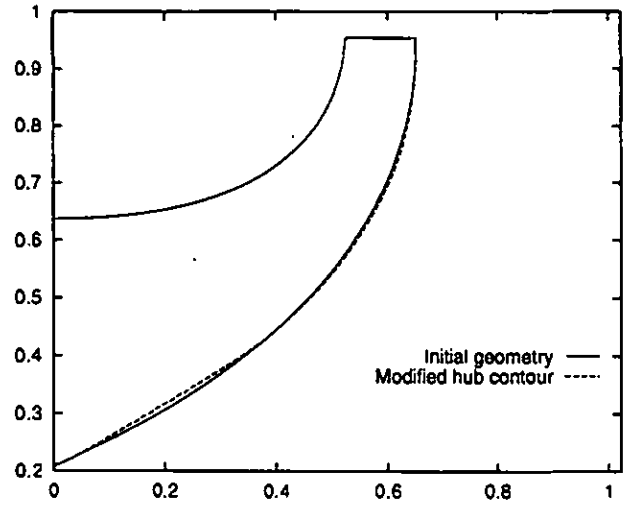


**Fig. 7: Hub contour modification**

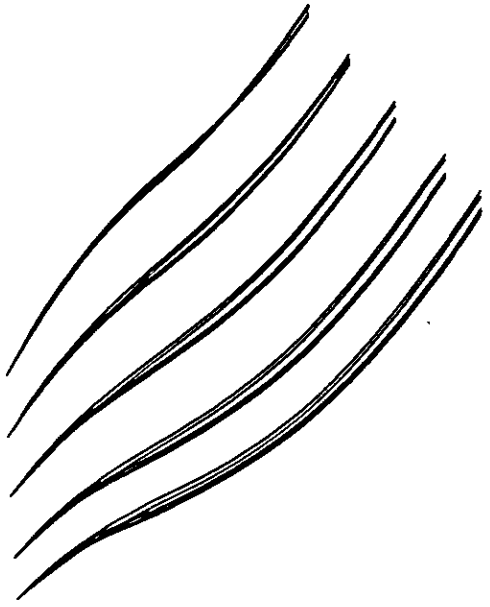

**Fig. 8: Initial (grey) and modified blade shapes - Superimposed view of 5 sections from hub (bottom) to shroud (top) in the $(m,r\theta)$ plane**

oscillations, that should be eliminated.

This impeller blade has been re-designed in three steps.

- The hub endwall has been modified, in order to reduce the flow deceleration occuring in the first half of the channel.
- Secondly the blade shape has been re-designed, to obtain a more gradual increase of blade loading.
- After these two steps, the mean velocity distribution

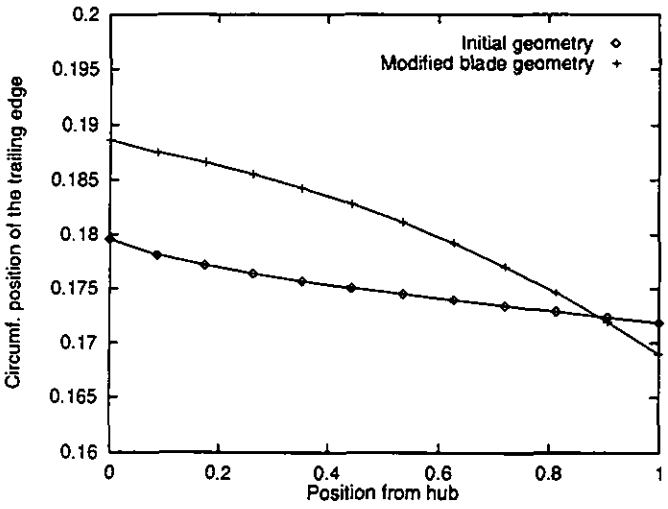


**Fig. 9: Trailing edge of the initial and modified blades**

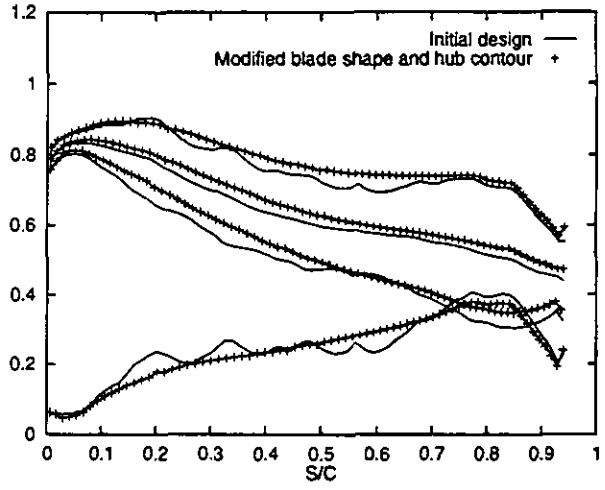


**Fig. 11: Isentropic Mach number and loading distributions around the initial and final designs - Tip section**

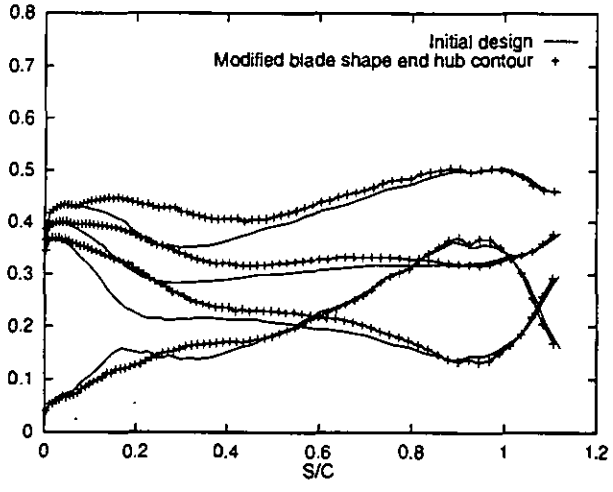


**Fig. 10: Isentropic Mach number and loading distributions around the initial and final designs - Hub section**

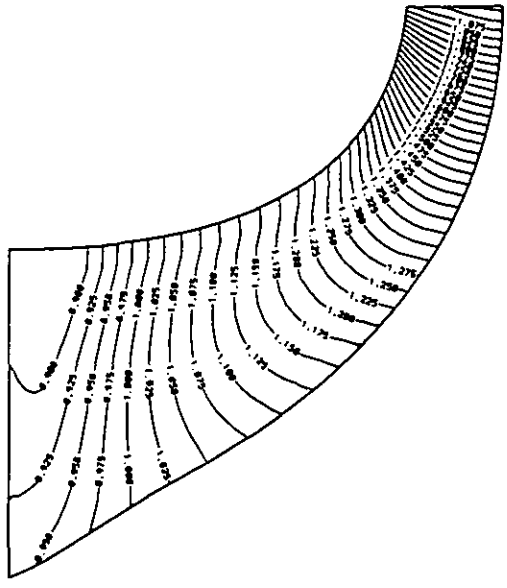

**Fig. 12: Circumf.-averaged pressure distribution in the channel - Modified design**

along the hub section of the blade was still showing an important deceleration, and the hub endwall was modified a second time.

The total modification of the hub endwall is shown in figure 7, and the initial and final blade shapes are compared on five equidistant sections from hub to tip in figure 8. The profiles are represented in the $(m, r\theta)$ plane, and have been (for the sake of clarity) gradually translated along the vertical direction (the leading edge of the blade is not leaned, and the profiles should therefore coincide at the leading edge). The most siginificant blade shape modifications are observed at the hub section (bottom of the figure).

In order to avoid the appearance of spurious oscillations of the blade shape in the spanwise direction, the target pressure distribution is imposed at 5 equidistant sections from hub to tip, and calculated by interpolation between these sections. The trailing edges of the initial and modified blades can be compared in figure 9, which compares the initial and modified distributions of the $r\theta$ coordinate along the spanwise direction. The new blade presents a larger spanwise variation, but should however still be manufacturable.

The isentropic Mach number distributions along the hub

and tip sections of the new geometry are compared to the initial ones in figures 10 and 11. Almost linear distributions of blade loading and mean velocity level have been achieved along the hub section. The tip loading distribution has also been improved, showing more monotonic variations, and a decreased loading near the exit.

As the outlet section has been slighly modified, the outlet static pressure has been iteratively modified during the design, in order to keep a constant mass flow, and hence an unchanged incidence on the blades. The spanwise distribution of outlet flow angle remained practically unchanged (differences of 0.5 degree in relative outlet flow angle have been observed). The iso-pressure lines in figure 12 show that a more constant compression rate is achieved along the endwalls.

## NAVIER-STOKES VERIFICATION

In this last section the results of the Navier-Stokes analyses of the initial and modified designs are presented.

The 3D Navier-Stokes computations have been performed with the Numeca FINE/TURBO solver for internal flows, whose validity in the prediction of the flow in centrifugal impellers has been demonstrated (Hirsch et al, 1996).

The method solves the three-dimensional Reynolds-averaged Navier-Stokes equations on multi-block structured grids. The computation of the advective and viscous terms is based on a cell-centered finite volume formulation. The multigrid approach ensures the efficiency of the code by providing fast convergence to steady state. In the computations presented hereafter the algebraic model of Baldwin-Lomax has been selected.

The mesh generation process has been performed with the Numeca's IGG/Autogrid (Interactive Geometry Modeller and Grid Generation System) software, which allows for a rapid and fully automatic meshing of turbomachinery components.

In the present simulations mono-block periodic H-type structured grids have been used to discretise both impellers, which was found to be consistent with the previous 3D Euler computations. The number of mesh points used was 129x33x33, for a total number of 135168 cells. A high stretching has been imposed along the walls, so that a correct capturing of the boundary layers was ensured (the non-dimensional distance of the first mesh line from the walls was of the order of 1). The leakage flow has been neglected, and the case of a shrouded impeller has been considered.

The computations have been performed in order to have the same mass flow of 7 kg/s through both impellers. The computed isentropic Mach number distributions are compared at hub and shroud in figure 13. Although it is always difficult to realise the same working conditions, the results clearly confirm the ones predicted by the inviscid calculations. The mean velocity distribution along the hub is more constant, and hence a lower amount of diffusion is created. Along the tip section the Mach number corresponding to the initial design rapidly decreases along the pressure side, this

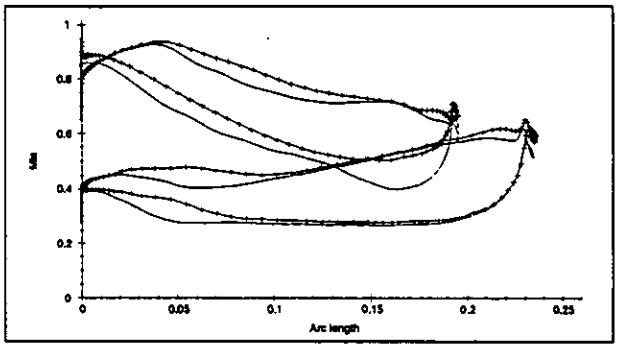


**Fig. 13: Navier-Stokes calculations - Initial (–) and modified (+) is. Mach number distributions along the hub and tip sections**

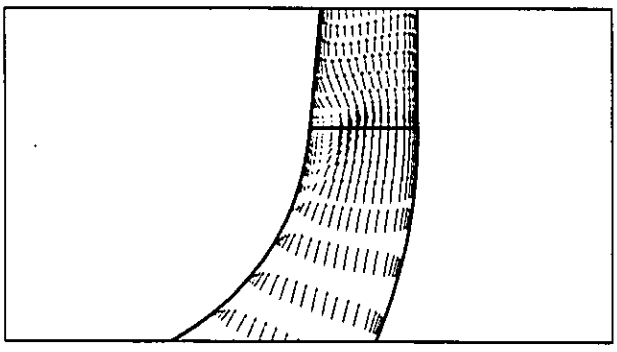

**Fig. 14: Initial design - Meridional projection of the velocity vectors on a grid surface close to the suction surface**

deceleration being less significant for the redesigned blade. This modification of blade loading at the rear part of the blade was underpredicted by the inviscid calculations. The incidence on the blades is slightly smaller than the one predicted by the inviscid calculations, which can be attributed to the endwall boundary layers blockage (neglected in the inviscid calculations). In order to improve the correspondence between the results, the mass flow should have been imposed at a slightly smaller value.

Although the number of mesh points used is probably insufficient for predicting accurately the efficiency, it is often accepted that results can be used for a comparative purpose. The efficiency of the impellers has been computed, comparing the total enthalpy rise to the isentropic one (calculated from the total pressure ratio). The calculated efficiency for the redesigned impeller is 89.5%, to be compared to 87.6% for the initial one. These results seem to indicate that the inverse method permitted to increase the real efficiency of the

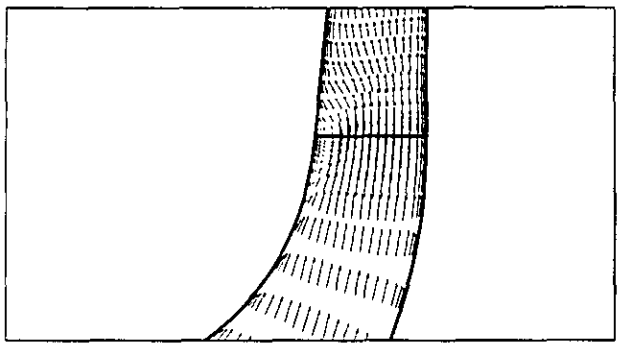

**Fig. 15: Modified design - Meridional projection of the velocity vectors on a grid surface close to the suction surface**

impeller. This gain of efficiency can probably be explained by the reduction of the size and intensity of the suction side separation predicted near the shroud. The figures 14 and 15 permit to observe that the size of the separation zone is clearly smaller in the case of the modified design.

## CONCLUSIONS

An inverse method has been used to improve the pressure field in a centrifugal impeller. The design method is based on Euler computations with moving boudaries. The blade design is made by means of the 3D inverse method, while the endwall design is based on a 'meridional' version of the method, solving the circumferentially-averaged Euler equations in the meridional plane.

It has been shown that the strategy consisting of modifying separately the hub contour and blade walls in order to control respectively the mean velocity and loading distributions is efficient.

An example has been presented, in which the hub endwall and the blades of a centrifugal impeller have been redesigned in order to reduce the amount of diffusion and to obtain a linear distribution of blade loading. Navier-Stokes computations have confirmed the inviscid prediction in terms of pressure distributions. An expected gain of 1.9% of efficiency has been calculated, that should be experimentally confirmed.

## REFERENCES


1. Casey, M.V., Dalbert, P., Roth, P., 1992, "The Use of 3D Viscous Flow Calculations in the Design and Analysis of Industrial Centrifugal Compressors", Journal of Turbomachinery, Vol. 114, pp 27-37.

2. Dang, T.Q., Nerurkar, A.C., Reddy, D.R. , 1997, "Design Modification of Rotor 67 by 3D Inverse Method - Inviscid Flow Limit", ASME Paper 97-GT-484.

3. Demeulenaere, A., and Van den Braembussche, R., 1996, "Three-Dimensional Inverse Method for Turbomachinery Blading Design", ASME Paper 96-GT-039.

4. Demeulenaere, A., Léonard, O.,1997, "A Navier-Stokes Inverse Method Based on a Moving Wall Strategy", ASME GT-97-416.

5. Demeulenare, A., 1997, "An Euler/Navier-Stokes Inverse Method for Compressor and Turhine Blade Design", von Karman Lecture Series on Inverse Design and Optimisation Methods, VKI LS 1997-05.

6. Eyi, S., Lee, K.D., Rogers, S.E., and Kwak, D., 1995, "High-Lift Design Optimization Using the Navier-Stokes Equations", AIAA 95-0477.

7. Giles, M., 1989, "Non Reflecting Boundary Conditions for Euler Equations Calculations", AIAA Journal, Vol. 108, No 12, pp 2050-2058.

8. Hawthorne, W.R., Tan C.S., Wang C. and McCune, J.E., 1984, "Theory of Blade Design for Large Deflections: Part I: Two-Dimensional Cascades", Transactions of the ASME, J. Eng. for Gas Turbines and Power, Vol. 106, No. 2, pp 346-353.

9. Hirsch, C., Kang, S. and Pointel, G., 1996, "A Numerically Supported Investigation of the 3D Flow in Centrifugal Impellers, Part I : The Validation Base", ASME Paper 96-GT-151.

10. Jameson, A., 1995, "The Present Status, Challenges, and Future Developments in Computational Fluid Dynamics", AGARD 77th Fluid Dynamics Panel Symposium, Seville.

11. Léonard, O. and Van den Braembussche, R., 1992a, "Design Method for Subsonic and Transonic Cascade with Prescribed Mach Number Distribution", Transactions of the ASME, Vol. 114, No. 3, pp 553-560.

12. Léonard, O. and Van den Braembussche, R., 1992b, "Inverse Design of Compressor and Turbine Blades at Transonic Flow Conditions", ASME Paper 92-GT-430.

13. Van den Braembussche, R., Demeulenaere, A., Borges, J., 1993, "Inverse Design of Radial Flow Impellers with Prescribed Velocity at Hub and Shroud", in *Technology Requirements for Small Gas Turbines*, Agard CP-537, pp 18-1:18-9.

14. Zangeneh, M., 1993, "Inviscid-Viscous Interaction Method for 3D Inverse Design of Centrifugal Impellers", ASME Paper 93-gt-103.

15. Zangeneh, M., 1997, "On the Design of Interstage Ducts, Diffuser Walls and Meridional Geometry of Turbomachines", ASME Paper 97-GT-208.